European Journal of Pharmaceutics and Biopharmaceutics 76 (2010) 10–16

Contents lists available at ScienceDirect

European Journal of Pharmaceutics and Biopharmaceutics

journal homepage: www.elsevier.com/locate/ejpb

Research paper

Folate-mediated poly(3-hydroxybutyrate-co-3-hydroxyoctanoate) nanoparticles for targeting drug delivery

Chan Zhang [a], LiangQi Zhao [a,*], YueFeng Dong [b], XiaoYan Zhang [a], Ji Lin [a], Zhang Chen [a]

[a] Key Laboratory of Chemical Biology and Molecular Engineering of Ministry of Education, Shanxi University, Taiyuan, PR China
[b] Institute of Medicine and Life Science of Shanxi Province, Taiyuan, PR China

ARTICLE INFO

Article history:
Received 22 March 2010
Accepted in revised form 10 May 2010
Available online 22 May 2010

Keywords:
Targeting drug delivery system
Poly(3-hydroxybutyrate-co-3-hydroxyoctanoate)
Doxorubicin
Nanoparticles

ABSTRACT

A novel targeting drug delivery system (TDDS) has been developed. Such a TDDS was prepared by $W_1/O/W_2$ solvent extraction/evaporation method, adopting poly(3-hydroxybutyrate-co-3-hydroxyoctanoate) [P(HB-HO)] as the drug carrier, folic acid (FA) as the targeting ligand, and doxorubicin (DOX) as the model anticancer drug. The average size, drug loading capacity and encapsulation efficiency of the prepared DOX-loaded, folate-mediated P(HB-HO) nanoparticles (DOX/FA–PEG–P(HB-HO) NPs) were found to be around 240 nm, 29.6% and 83.5%. The *in vitro* release profile displayed that nearly 50% DOX was released in the first 5 days. The intracellular uptake tests of the nanoparticles (NPs) *in vitro* showed that the DOX/FA–PEG–P(HB-HO) NPs were more efficiently taken up by HeLa cells compared to non-folate-mediated P(HB-HO) NPs. In addition, DOX/FA–PEG–P(HB-HO) NPs (IC_{50} = 0.87 μM) showed greater cytotoxicity to HeLa cells than other treated groups. *In vivo* anti-tumor activity of the DOX/FA–PEG–P(HB-HO) NPs showed a much better therapeutic efficacy in inhibiting tumor growth, and the final mean tumor volume was 178.91 ± 17.43 mm^3, significantly smaller than normal saline control group (542.58 ± 45.19 mm^3). All these results have illustrated that our techniques for the preparing of DOX/FA–PEG–P(HB-HO) NPs developed in present work are feasible and these NPs are effective in selective delivery of anticancer drug to the folate receptor-overexpressed cancer cells. The new TDDS may be a competent candidate in application in targeting treatment of cancers.

1. Introduction

Conventional chemotherapy, owing to its non-specific delivery of anticancer drugs to both normal and cancer cells, often has severe side effects to the cancer patients being taken chemotherapy [1]. It would be an intriguing situation if we utilize those anticancer drugs being able to target cancer cells specifically, and then the side effects would be drastically decreased. Thus, targeting delivery of anticancer drugs is preferred and it has been explored intensively in recent decades [2–5]. Targeting drug delivery system (TDDS) mainly composed of targeting ligand, carrier and model drug may fulfill many attributes of a 'magic bullet' [6].

A common phenomenon was reported repeatedly by numerous works, i.e. a remarkable overexpression of the epidermal growth factor receptor [7], transferrin receptor [8,9] and folate receptor [10,11] had been observed in many kinds of human cancers. Among these receptors, folate receptor (FR) is a glycosylphosphatidylinositol-anchored glycoprotein, with an apparent molecular weight of 38–40 kDa [12,13]. Its correspondence, folic acid (Folate, FA), has widely been used as a targeting ligand to deliver therapeutic agents to cancer cells due to its high binding affinity for FR ($K_d \sim 10^{-10}$ M) [14–16]. Studies have found that NPs, liposomes and micelles of biodegradable polymers (such as PLGA, PLA–TPGS, MPEG–PCL, DSPE–PEG) use FA as a targeting ligand [17–23]. However, publications on the modification of polyhydroxyalkanoates (PHAs) via covalent bonding of FA and its application have not been seen up to now.

PHAs, a class of versatile biodegradable and biocompatible materials, have attracted much attention of scientists in biomedical fields. It has been a veteran in bone tissue engineering applications [24]. These polymers are also potential candidates as carriers in drug delivery systems due to their unique and interesting physicochemical features in addition to mechanical properties similar to those of polypropylene and polylactic-co-glycolic acids [25]. Poly(3-hydroxybutyrate-co-3-hydroxyoctanoate) [P(HB-HO)] is one of the latest PHAs prepared by *Sinorhizobium fredii* in our lab and its biodegradation and biocompatibility has been proved better than other members (e.g. PHB, PHBV) of PHAs [26–28]. Therefore, we think that such a polymer may have some advantages over other members in the applications of drug delivery.

* Corresponding author. Address: Key Laboratory of Chemical Biology and Molecular Engineering of Ministry of Education, Shanxi University, Taiyuan 030006, PR China. Tel.: +86 351 7017663; fax: +86 351 7011499.
E-mail addresses: zhang_chan@yahoo.com (C. Zhang), liangqi@sxu.edu.cn (L. Zhao).

0939-6411/$ - see front matter Crown Copyright © 2010 Published by Elsevier B.V. All rights reserved.
doi:10.1016/j.ejpb.2010.05.005

The aim of the present work is to construct a new and biocompatible TDDS based on the high affinity of FA and FR. We have synthesized a novel folic acid conjugate, FA–PEG–P(HB-HO) and its chemical structure was characterized by FTIR and ^{1}H NMR methods. Doxorubicin (DOX) was adopted as a model anticancer drug, which is an effective and widely used anticancer agent in different cancers [29–31]. DOX-loaded folate-mediated P(HB-HO) nanoparticles (DOX/FA–PEG–P(HB-HO) NPs) were prepared by FA–PEG–P(HB-HO), and their physicochemical properties, including particle size, surface morphology, drug loading capacity, encapsulation efficiency and *in vitro* release, were investigated. And the pharmacodynamics of DOX/FA–PEG–P(HB-HO) NPs was also investigated by the experiments of *in vitro* cellular uptaking, *in vitro* cytotoxicity and *in vivo* anti-tumor activity.

2. Materials and methods

2.1. Materials

Poly (3-hydroxybutyrate-co-3-hydroxyoctanoate) [P(HB-HO)] (average molecular weight, M_w 1.85 × 10^5 Da) containing 10% molar of 3-hydroxyoctanoate units was fermented from *S. fredii* in our laboratory. Doxorubicin was bought from Wanle pharmaceuticals Inc. (Shenzhen, China). Folic acid (FA), polyoxyethylene-bis-amine (H_2N–PEG–NH_2, M_w 3350), *N*,*N*′-dicyclohexylcarbodiimide (DCC), pyridine, 3-(4,5-dimethylthiazol-2-yl)-2,5-diphenyl tetrazolium bromide (MTT) and RPMI-1640 medium without folic acid were products of Sigma–Aldrich (St. Louis, MO, USA). Fetal bovine serum (FBS) was purchased from Gibco (Life Technologies, AG, Switzerland). All reagents and solvents were of analytical or HPLC grade and used without further purification. Millipore water was produced by the Milli-Q Plus System (Millipore Corporation, Breford, USA).

HeLa cells, a human cervical carcinoma cell line, were provided by Cell Bank of Chinese Academy of Sciences.

2.2. Synthesis of FA–PEG–P(HB-HO)

FA–PEG–P(HB-HO) was synthesized by the following procedures:

First, the amination of FA was carried out using the literature method with some modifications [32,33]. To synthesize FA–PEG–NH_2, the reactants, FA, H_2N–PEG–NH_2, DCC and Pyridine were dissolved in DMSO. The reaction mixture was kept stirring overnight in the dark at room temperature. The product was centrifuged to remove away the by-product, dicyclohexyl urea (DCU). The supernatant was dialyzed against Milli-Q water at 4 °C to remove DMSO and unreacted folic acid. The trace amount of unreacted H_2N–PEG–NH_2 was then removed by batch-adsorption with cellulose phosphate cation-exchange resin. The resultant product was obtained by freeze drying.

Second, to synthesize FA–PEG–P(HB–HO), FA–PEG–NH_2 and P(HB-HO) were reacted in chloroform overnight at room temperature with DCC and pyridine as catalysts. The solvent was then removed on a rotary evaporator, and the product was suspended in 50 mM Na_2CO_3. These were dialyzed against Milli-Q water and purified on a DEAE-trisacryl Sepharose column to remove by-products. The product was then lyophilized to yield a yellow dry powder.

2.3. Preparation of DOX/FA–PEG–P(HB-HO) NPs

DOX/FA–PEG–P(HB-HO) NPs were prepared by a modified W_1/O/W_2 solvent extraction/evaporation method [34,35]. For DOX/FA–PEG–P(HB-HO) NPs, in brief, DOX in aqueous solution (W_1) was emulsified in a solution of FA–PEG–P(HB-HO) with Tween80 and Span80 in chloroform (O) using a sonicator. This primary emulsion W_1/O was then added to an aqueous phase (W_2) containing PVA as emulsifier, which was sonicated again. The resultant double emulsion was stirred overnight to allow the organic solvent to evaporate. The particle suspension was centrifuged at 15,000 rpm for 30 min. The sample was washed with Milli-Q water repeatedly and freeze-dried to get the NPs powder.

The blank P(HB-HO) NPs and blank FA–PEG–P(HB-HO) NPs were made by the same method except taking an aqueous solution without DOX as W_1. The DOX/P(HB-HO) NPs were prepared by the same method, only except using P(HB-HO) instead of FA–PEG–P(HB-HO).

2.4. Characterization

2.4.1. Characterization of FA–PEG–P(HB-HO)

The chemical structure of the synthesized FA–PEG–P(HB-HO) was characterized by FTIR spectroscopy (FTIR-8300, Shimadzu, Japan) and ^{1}H NMR spectroscopy (DRX-300, Bruker, Switzerland).

2.4.2. Particle size and size distribution

Average particle size and size distribution of the DOX/FA–PEG–P(HB-HO) NPs were determined on a laser particle size analyzer (Eye Tech, Ankersmid Ltd., Holland). The NPs were diluted with Milli-Q water and sonicated for 3 min before measurement.

2.4.3. Scanning electron microscopy

The surface morphology of the DOX/FA–PEG–P(HB-HO) NPs was observed by scanning electron microscopy (JEOL JSM-35C, Tokyo, Japan) after the samples being gold coated, and digital images were processed using Adobe Photoshop and Image-J software.

2.4.4. Drug loading (DL) and encapsulation efficiency (EE)

The NPs were dissolved in a mixed solution of chloroform and methanol (v/v 3:1). The quantity of DOX loaded in the NPs was determined on a UV–Vis spectrophotometer (U-2010 spectrophotometer, Hitachi, Japan) by measuring the UV absorbance at λ = 498.5 nm. The DL and EE were calculated as follows:

$$\mathrm{DL} = (\text{weight of DOX in NPs}/\text{weight of DOX-loaded NPs}) \times 100$$

$$\mathrm{EE} = (\text{weight of DOX in NPs}/\text{theoretical weight of DOX}) \times 100$$

2.4.5. In vitro release studies

The release of DOX from the drug-loaded NPs was carried out in an incubator shaker (HZ-9301K, China) at 100 rpm and 37 ± 1 °C. A dynamic dialysis technique was employed. Practically, 100 mg of drug-loaded NPs were put in a pretreated dialysis bag with 10 mL PBS (pH 7.4). The dialysis bag was sealed and suspended in 100 mL PBS (pH 7.4) to ensure an immersed condition. At various time intervals, samples of 5 mL were collected and replaced by an equal volume of fresh buffer. Then, the samples were centrifuged at 10,000 rpm for 10 min (CR22G high-speed refrigerated centrifuge, Hitachi, Japan). The amount of DOX in the supernatant was determined at 480 nm excitation and 580 nm emission on the fluorescence spectrophotometer (F-2500, Hitachi, Japan). Triplicate measurements were performed for each time.

2.4.6. Stability of DOX/FA–PEG–P(HB-HO) NPs

To determine the stability of DOX/FA–PEG–P(HB-HO) NPs, they were stored in powder form at 4 °C for 6 months. And then, the properties of the NPs, including particle size, DL and EE, were analyzed as described previously.

2.5. Cell line experiment

2.5.1. Cell culture

HeLa cells that overexpress folate receptor were provided from Cell Bank of Chinese Academy of Sciences. RMPI 1640 medium without folic acid was used for HeLa cells and was supplemented with 10% FBS and 1% antibiotics. Cells were cultivated in medium at 37 °C in humidified environment of 5% CO_2. Before the *in vitro* experiments, the cells were pre-cultured until confluence was reached.

2.5.2. In vitro cellular uptake of NPs

HeLa cells were seeded in 6-well plates. After the cells reached 70–80% confluency, they were incubated with 5 μM DOX/FA–PEG–P(HB-HO) NPs or DOX/P(HB-HO) NPs for 4 h at 37 °C and the cells were washed three times with cold PBS after incubation. An aliquot of the cells was examined on a Olympus fluorescence microscope (BX51, Olympus, Japan), the rest part of the cells was lysed in 0.5 mL PBS containing 1% Triton X-100, the fluorescence intensity of the cellular lysate was measured at 480 nm excitation and 580 nm emission on the fluorescence spectrophotometer (F-2500, Hitachi, Japan).

2.5.3. In vitro cytotoxicity tests

The *in vitro* cytotoxicity was investigated by MTT assay [36,37]. HeLa cells were incubated in 96-well plate at 5×10^4 cells per well, and followed by incubation for 24 h. The culture medium was then replaced with an equal volume of fresh medium containing different drug formulations in blank P(HB-HO) NPs, blank FA–PEG–P(HB-HO) NPs, free DOX, DOX/P(HB-HO) NPs, DOX/FA–PEG–P(HB-HO) NPs and DOX/FA–PEG–P(HB-HO) NPs with 1 mM free folic acid. All of the samples were UV sterilized. After 12 h incubation, the cells were washed twice with PBS and cultured in fresh medium for 24 h. Then, 20 μL MTT solution (5 mg/mL in PBS, pH 7.4) was added to the wells, and followed by further incubation for 4 h. Thereafter, the media was removed, and the formazan crystals formed were dissolved in dimethyl sulfoxide (DMSO) (200 μL/well), and the absorbance was obtained at 570 nm on an ELISA reader (Bio-Rad550, USA). The sample-free wells were used as the control. Data were averaged from the eight different wells per condition and plotted as mean ± standard error.

2.6. Assessment of anti-tumor activity

All animal procedures were performed in compliance with the guidelines for the care and use of experimental animals, which had been drawn up by the Committee for Animal Experimentation of the National Cancer Center. All guidelines met the ethical standards required by the law and also complied with the guidelines for the use of experimental animals in China.

Female BALB/c nude mice (4–6 weeks of age, the Institute of Laboratory Animal Science, Chinese Academy of Medical Sciences, Beijing, China) were maintained on a folate-deficient rodent diet and in a pathogen-free condition on arrival. To generate HeLa tumor xenografts, 1×10^7 cells suspended in 20 μL of normal saline were inoculated into the right limb armpits of the mice. After 10 days, when the average volume of the xenograft tumors reached 50 mm^3, the mice were randomly divided into five groups, each group having six mice. Various formulations of DOX (group I: normal saline; group II: free DOX; group III: DOX/P(HB-HO) NPs; group IV: DOX/FA–PEG–P(HB-HO) NPs; group V: DOX/FA–PEG–P(HB-HO) NPs + 1 mM free folic acid) were injected intravenously via the tail vein every two days for a total of four times. The amounts of DOX administered were 5 mg/kg in all of the formulations. Tumors were measured with a caliper at a frequency of every 3 days, and the tumor volume (V) was calculated as $V = \pi ab^2/6$, here a = major axis, b = minor axis. Tumor volume is shown as the mean ± standard error.

3. Results and discussion

3.1. Synthesis and characterization of FA–PEG–P(HB-HO)

The principle of the chemical reactions in synthesis of FA–PEG–P(HB-HO) is the formation of amide bonds. The conditions of synthesizing FA–PEG–NH_2 were as follows: the molar ratio of

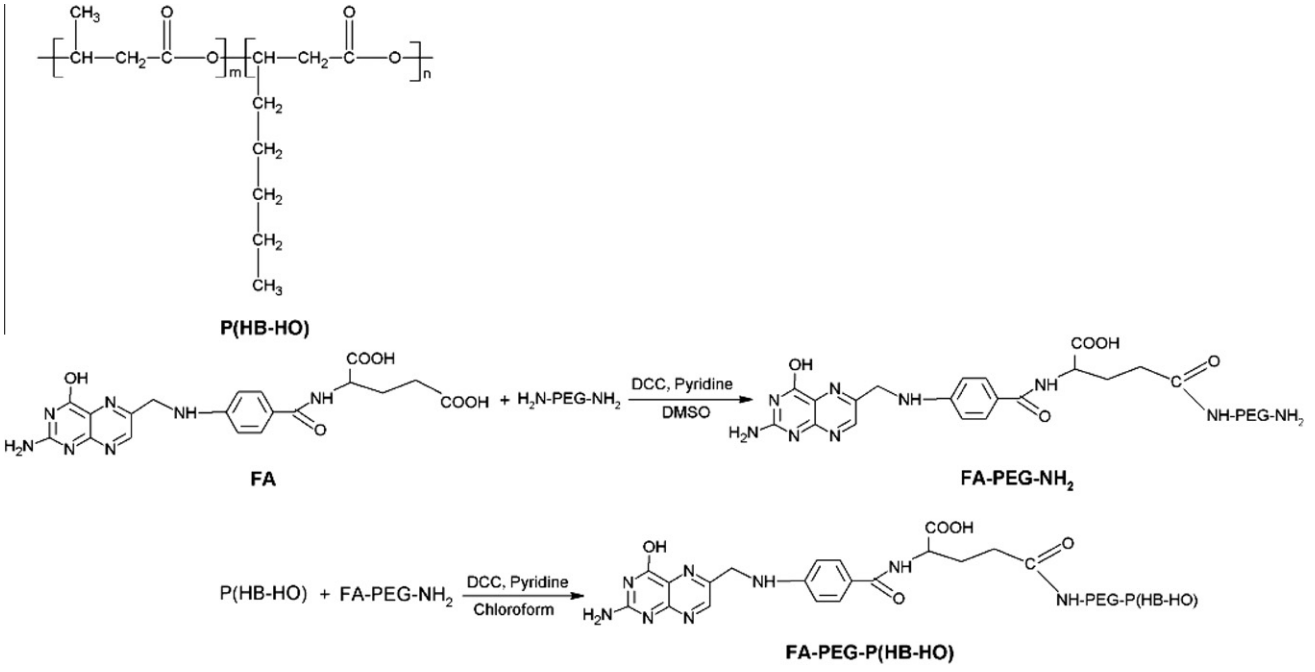

Fig. 1. Synthesis of FA–PEG–P(HB-HO) conjugate.

FA:H_2N–PEG–NH_2:DCC:Pyridine was 1:1:1:1. The optimal conditions of synthesizing FA–PEG–P(HB-HO) were the molar ratio of FA–PEG–NH_2:P(HB-HO):DCC was 1:1:1. The process of synthesizing FA–PEG–P(HB-HO) was illustrated in Fig. 1.

The conjugate structure was checked and confirmed by FTIR and ^{1}H NMR spectroscopy as shown in Fig. 2. FTIR spectrum quantitatively confirmed the conjugation by several characteristic vibrational modes. More specifically, the bands at ~1101 cm^{-1} and 1724 cm^{-1} were assigned to C–O–C ether stretching vibration of NH_2–PEG–NH_2 and –COO stretching vibration of P(HB-HO), respectively. The band at 1454 cm^{-1} was attributed to characteristic absorption band of the phenyl ring in folic acid. The absorption bands at 3438 cm^{-1} and 1633 cm^{-1} were due to the NH-stretching and C=O stretching vibrations of –$CONH_2$ group. ^{1}H NMR analysis showed principal peaks (in ppm) related to the folate moiety [δ = 8.63, 7.66, 6.62, 4.52, 3.38, 1.92 ppm], the PEG moiety [δ = 3.64 ppm], and the P(HB-HO) moiety [δ = 5.25, 2.52, 1.61, 1.25, 1.05, 0.9 ppm].

3.2. Preparation and characterization of DOX/FA–PEG–P(HB-HO) NPs

3.2.1. Preparation of DOX/FA–PEG–P(HB-HO) NPs

Based on previous experiments, the correlative parameters of $W_1/O/W_2$ solvent extraction/evaporation method were optimized. And the optimal conditions were as follows: the concentration of FA–PEG–P(HB-HO), DOX, Tween80, Span80 and PVA were 6.5%, 10%, 5%, 1% and 3% (W/V), separately. The ultrasonic time and output was 180 s and 200 W, respectively.

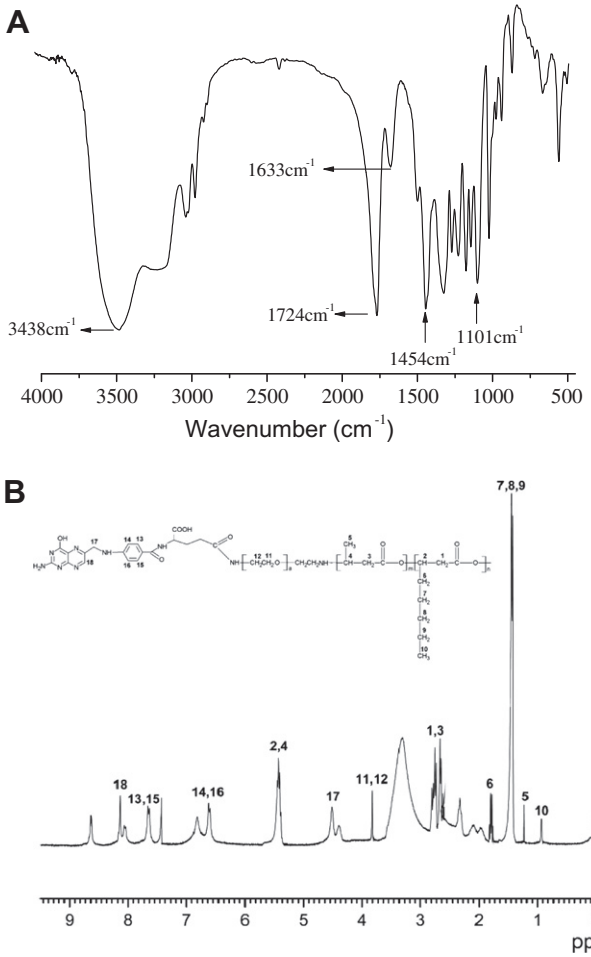

Fig. 2. The FTIR spectrum (A) and ^{1}H NMR spectrum (B) of FA–PEG–P(HB-HO).

3.2.2. Particle size and size distribution

The size and size distribution of the NPs were measured using a laser particle size analyzer and are listed in Table 1. It can be observed that the diameters of the two formulations are in the range of 200–300 nm with polydispersity of 0.2–0.4.

3.2.3. Scanning electron microscopy

From the SEM image of the DOX/FA–PEG–P(HB-HO) NPs shown in Fig. 3, it can be seen that the NPs are spherical in shape and have a size distribution approximately from 200 to 300 nm. The particle size observed is in good agreement with the value determined by laser particle size analyzer.

3.2.4. Drug loading (DL) and encapsulation efficiency (EE)

Table 1 shows the DL and EE of the two formulations, namely DOX/P(HB-HO) NPs and DOX/FA–PEG–P(HB-HO) NPs. Both DL and EE were influenced by the changes of initial weight ratio of

Table 1
Characteristics of DOX/P(HB-HO) NPs and DOX/FA–PEG–P(HB-HO) NPs (n = 3).

NPs	Characteristics	0 month	6 months
DOX/P(HB-HO) NPs	Particle size (nm)	223.2 ± 5.1	243.4 ± 4.9
	Polydispersity	0.33 ± 0.02	0.41 ± 0.04
	DL (%)	27.4 ± 3.4	25.3 ± 4.6
	EE (%)	80.8 ± 4.5	71.5 ± 3.8
DOX/FA–PEG–P(HB-HO) NPs	Particle size (nm)	241.6 ± 9.3	257.3 ± 8.6
	Polydispersity	0.24 ± 0.04	0.30 ± 0.02
	DL (%)	29.6 ± 2.9	27.7 ± 3.4
	EE (%)	83.5 ± 5.7	76.1 ± 6.2

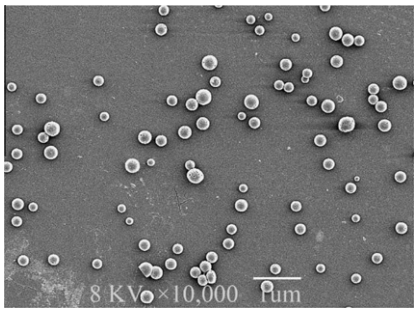

Fig. 3. SEM image of DOX/FA–PEG–P(HB-HO) NPs.

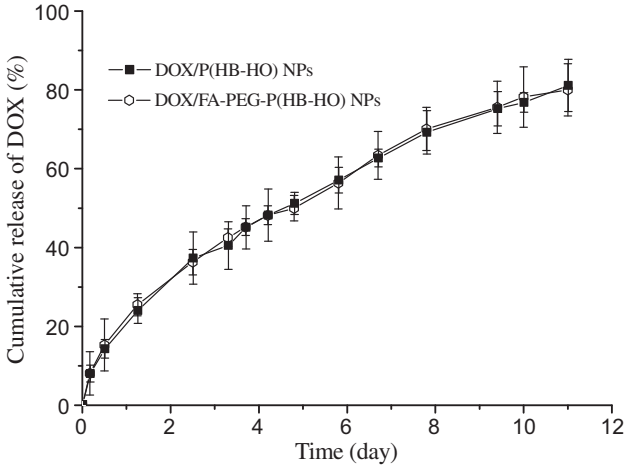

Fig. 4. The release profile of DOX/P(HB-HO) NPs and DOX/FA–PEG–P(HB-HO) NPs in pH 7.4 PBS.

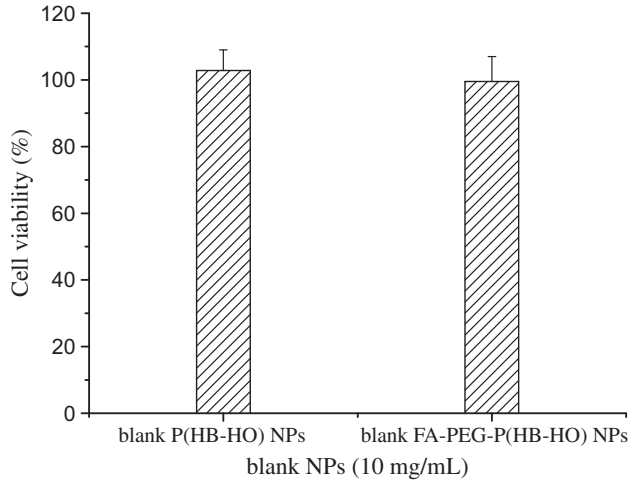

Fig. 5. Cell cytotoxicity results for blank P(HB-HO) NPs and blank FA–PEG–P(HB-HO) NPs.

drug to the copolymer (data not shown) and the optimal ratio was found to be 1:2 with 29.6% DL and 83.5% EE for DOX/FA–PEG–P(HB-HO) NPs.

3.2.5. In vitro drug release

The *in vitro* drug release profiles are shown in Fig. 4. During the first day, the DOX release rate exhibited a small burst release which accounted for less than 20% of the total drug encapsulated. The initial burst release can be attributed to DOX molecules located within the concave or on the surface of drug-loaded NPs. Nearly 50% DOX was released in the first 5 days.

3.2.6. Stability of DOX/FA–PEG–P(HB-HO) NPs

As shown in Table 1, the mean particle size of DOX/FA–PEG–P(HB-HO) NPs increased from 241.6 to 257.3 nm, and the EE was reduced to 76.1% when stored for 6 months at 4 °C. There were no great changes in the properties of the NPs. Therefore, these data suggest DOX/FA–PEG–P(HB-HO) NPs have excellent stability.

Table 2
Cytotoxicity of DOX/FA–PEG–P(HB-HO) NPs in HeLa cells determined by MTT assay.

Group	IC_{50} (μM)
Free DOX	2.8 ± 0.4
DOX/P(HB-HO) NPs	27.53 ± 1.9
DOX/FA–PEG–P(HB-HO) NPs	0.87 ± 0.05
DOX/FA–PEG–P(HB-HO) NPs + 1 mM folic acid	7.21 ± 0.3

3.3. In vitro cytotoxicity

Cytotoxicity of DOX/FA–PEG–P(HB-HO) NPs was evaluated by an MTT assay in HeLa cells. The cell viability (%) in the presence of blank P(HB-HO) NPs and blank FA–PEG–P(HB-HO) NPs was 102.8 ± 6.2% and 99.5 ± 7.5% (Fig. 5). The results demonstrated that no toxicity was observed after incubation with the two NPs, and the two polymers displayed satisfactory biocompatibility. As shown in Table 2, the IC_{50} of DOX/FA–PEG–P(HB-HO) NPs was 0.87 μM, which was 32 times lower than that of DOX/P(HB-HO) NPs, but only 8.3 and 3.2 times lower than DOX/FA–PEG–P(HB-HO) NPs with 1 mM free folic acid and free DOX, respectively. The two DOX-encapsulated NPs showed a comparable cytotoxicity to free DOX [22]. As a small molecule, free DOX should diffuse into the cells very quickly [33]. The incubation time of HeLa cells with drug formulations was 12 h, at such a time scale, the free DOX had diffused into the cells close completely, while for DOX/P(HB-HO) NPs, drug diffusion was retarded at certain extent, not so obvious to be tested. Compared with DOX/P(HB-HO) NPs, the overexpression of FRs on the surface of HeLa cells may significantly enhance the uptake of the DOX/FA–PEG–P(HB-HO) NPs via FR-mediated endocytosis [38] and result in higher cytotoxicity. However, the presence of 1 mM folic acid may occupy the targeting site of HeLa

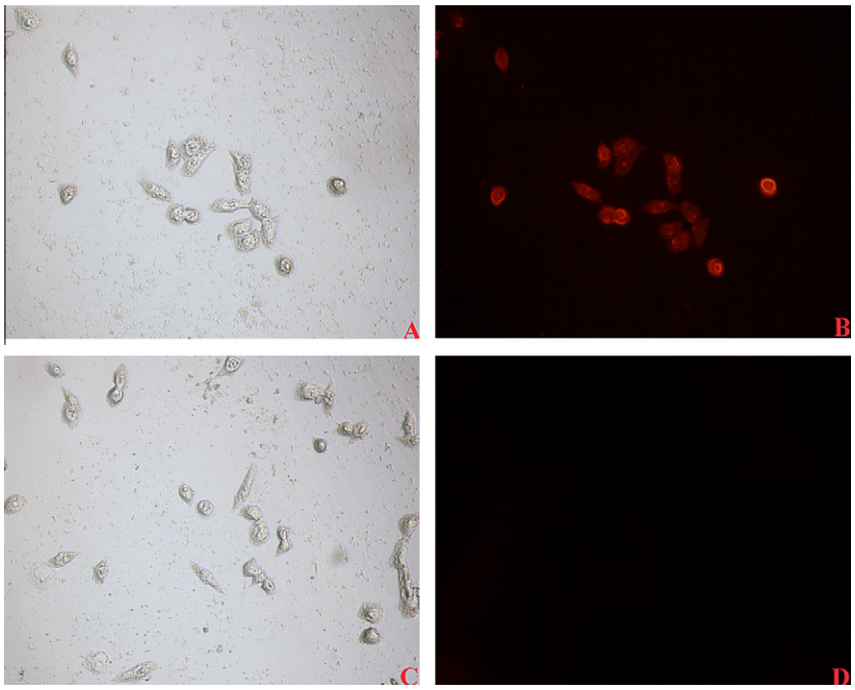

Fig. 6. Fluorescence observation of the uptake of DOX/FA–PEG–P(HB-HO) NPs and DOX/P(HB-HO) NPs by HeLa cells. HeLa cells were treated with DOX/FA–PEG–P(HB-HO) NPs and DOX/P(HB-HO) NPs. Left panels indicate cells visualized in the phase-contrast mode; Right panels indicate cells visualized in the fluorescence mode. Panels A and B, cells treated with DOX/FA–PEG–P(HB-HO) NPs; Panels C and D, cells treated with DOX/P(HB-HO) NPs. (For interpretation of the references to colour in this figure legend, the reader is referred to the web version of this article.)

cells and block the endocytosis of DOX/FA–PEG–P(HB-HO) NPs. Consequently, it is necessary to prepare the FR-mediated DOX/FA–PEG–P(HB-HO) NPs due to reducing dosages of drugs and improving therapeutic efficacy.

3.4. In vitro cellular uptake of NPs

The HeLa cells have a high level of the FR on their surface [32,39]. Uptake of DOX/P(HB-HO) NPs or DOX/FA–PEG–P(HB-HO) NPs by HeLa cells was analyzed by fluorescence microscope and fluorescence spectrophotometer. As shown in Fig. 6, DOX/FA–PEG–P(HB-HO) NPs were more efficiently taken up by the cells compared to non-targeted DOX/P(HB-HO) NPs. Similarly, intensity of fluorescence results showed that the cellular uptake of DOX/FA–PEG–P(HB-HO) NPs was about nine times higher than that of DOX/P(HB-HO) NPs (Fig. 7). These data demonstrated that DOX/FA–PEG–P(HB-HO) NPs could effectively target the HeLa cells through the FR.

3.5. In vivo anti-tumor activity

In vivo anti-tumor activity of DOX/FA–PEG–P(HB-HO) NPs was evaluated in BALB/c nude mice bearing HeLa tumor. As shown in Fig. 8A, all the treated groups suppressed the growth rate of tumor after injection of various formulations when compared with the normal saline control group; however, tumor volumes of each group changed differently. Owing to sustained release behavior of DOX/P(HB-HO) NPs, the tumor volume of DOX/P(HB-HO) NPs group was smaller than that of free DOX only with lower half-life. For the new system of present study, DOX/FA–PEG–P(HB-HO) NPs resulted in a significant anti-tumor efficacy, with a higher regression of the established tumors in nude mouse models. And the final mean tumor load was $178.91 \pm 17.43\ mm^3$, remarkably smaller than other treated groups. We think that delivery of DOX to the tumor cells had been enhanced due to the binding of FA to the nanoparticles. However, the uptake of DOX/FA–PEG–P(HB-HO) NPs could be blocked by 1 mM free folic acid. It is a reasonable inference that DOX/FA–PEG–P(HB-HO) NPs can be qualified as a good drug delivery system to suppress the tumor growth rate due to the targeting capability of folic acid as well as the suitable diameter of the nanoparticles. The higher cytotoxicity of DOX/FA–PEG–P(HB-HO) NPs to cancer cells than other treated groups *in vitro*

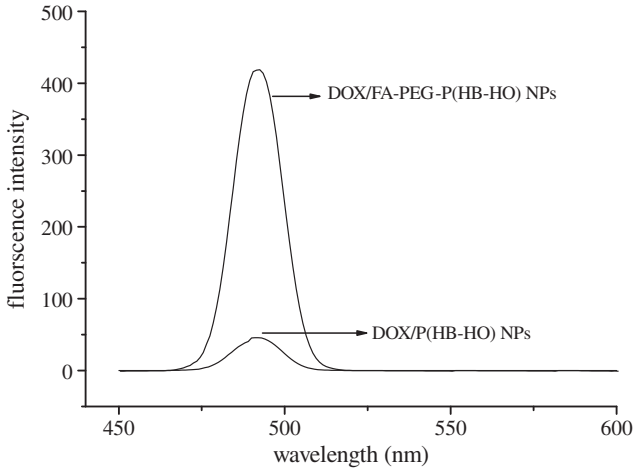

Fig. 7. Uptake of DOX/P(HB-HO) NPs and DOX/FA–PEG–P(HB-HO) NPs by HeLa cells measured by fluorescence spectrophotometer. The cells were incubated with DOX/P(HB-HO) NPs and DOX/FA–PEG–P(HB-HO) NPs for 4 h at 37 °C, washed with PBS and lysed in 1% Triton X-100 and measured for DOX fluorescence, as described in Section 2.5.2.

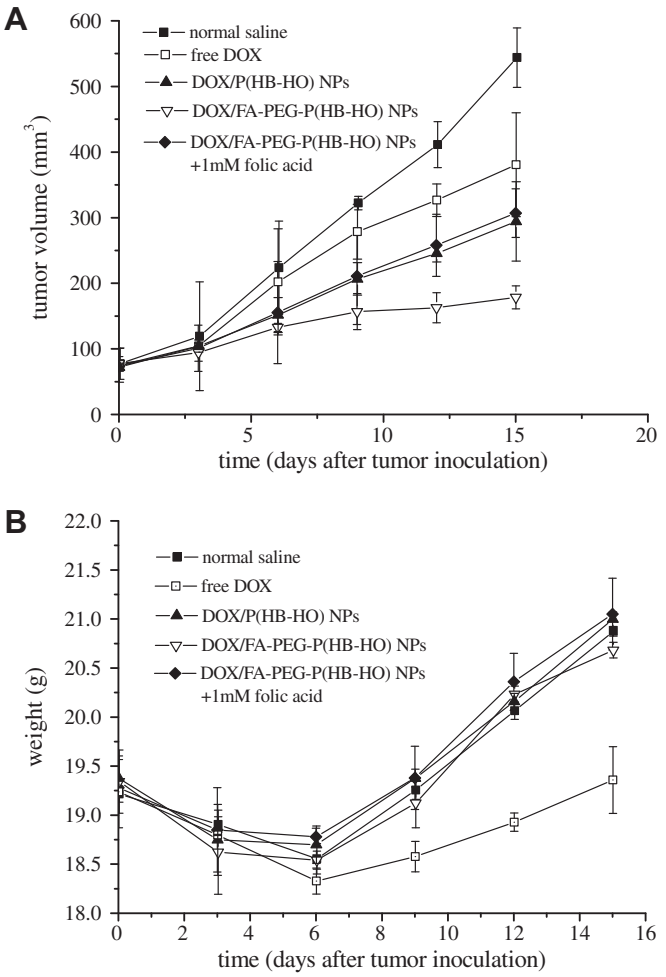

Fig. 8. Tumor volume changes (A) and body weight changes (B) of BALB/c nude mice bearing HeLa tumors after intravenous injections of various formulations of DOX ($n = 6$).

as shown in Table 2 in this study supports or coincides with the *in vivo* anti-tumor activity. The body weight changes of group I, III, IV and V were very stable (the up-curves in Fig. 8B). In the case of free DOX, however, a serious body weight decrease was observed due to its toxic side effects [40] (the bottom curve in Fig. 8B). All mice survived till the end of test period, and no fatal toxicity for normal growing was observed in the mice treated with the NPs formulations of DOX.

Fig. 9 shows the representative photographs of each group's tumor after the anti-tumor activity experiment, more specifically, the

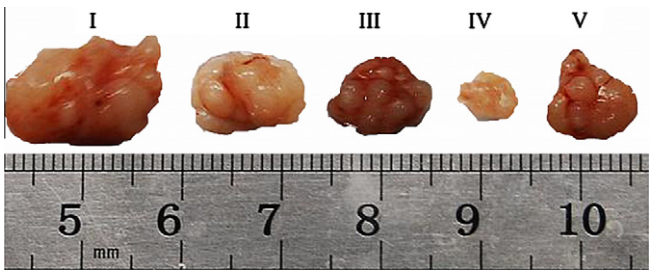

Fig. 9. Representative photographs of each group's tumor. I: normal saline; II: free DOX; III: DOX/P(HB-HO) NPs; IV: DOX/FA–PEG–P(HB-HO) NPs; V: DOX/FA–PEG–P(HB-HO) NPs + 1 mM free folic acid. (For interpretation of the references to colour in this figure legend, the reader is referred to the web version of this article.)

mice were killed and the tumors were picked out and their sizes were measured. The results showed that the tumor from DOX/FA–PEG–P(HB-HO) NPs-injected mice was the smallest among tested samples, followed by DOX/P(HB-HO) NPs, DOX/FA–PEG–P(HB-HO) NPs + 1 mM free folic acid, free DOX, and normal saline group.

From the above results, we can conclude with satisfaction that DOX-loaded, folate-mediated P(HB-HO) NPs bind to and internalize in tumor cells via FA–FR interactions, resulting a potent anti-tumor activity together with an accompanied decrease of toxic side effects. More detailed investigations into tissue distribution and pharmacokinetic properties are under further study.

4. Conclusions

In this paper, we have developed a new TDDS. We have synthesized an original FA–PEG–P(HB-HO) conjugate and confirmed its chemical structure by FTIR and ^{1}H NMR spectroscopy. DOX/FA–PEG–P(HB-HO) NPs were then prepared for targeting delivery of DOX to HeLa cancer cells. The average size of such NPs was found to be around 240 nm. Results on the experiments of intracellular uptake and *in vitro* cytotoxicity showed that the DOX/FA–PEG–P(HB-HO) NPs could focus to the HeLa cells efficiently and lead to a strong cytotoxicity due to high affinity of FA and FR. *In vivo* anti-tumor activity showed a much better therapeutic efficacy in inhibiting tumor growth. All these results have illustrated that the novel techniques for the preparation of DOX/FA–PEG–P(HB-HO) NPs developed in this work are feasible, and these NPs are effective in selective delivery of anticancer drug to the FR-overexpressed cancer cells. They are competent candidates to be applied in targeting treatment of cancers.

Acknowledgement

We are grateful to the financial support from the National Natural Science Foundation of China (Grant No. 50573045).

Appendix A. Supplementary data

Supplementary data associated with this article can be found, in the online version, at doi:10.1016/j.ejpb.2010.05.005.

References

[1] S. Wang, P.S. Low, Folate-mediated targeting of antineoplastic drugs, imaging agents, and nucleic acids to cancer cells, J. Control. Release 53 (1998) 39–48.
[2] S. Jaracz, J. Chen, L.V. Kuznetsova, I. Ojima, Recent advances in tumor targeting anticancer drug conjugates, Bioorg. Med. Chem. 13 (2005) 5043–5054.
[3] D. Hallahan, L. Geng, S.M. Qu, C. Scarfone, T. Giorgio, E. Donnelly, X. Gao, J. Clanton, Integrin-mediated targeting of drug delivery to irradiated tumor blood vessels, Cancer Cell 3 (2003) 63–74.
[4] J.M. Saul, A. Annapragada, J.V. Natarajan, R.V. Bellamkonda, Controlled targeting of liposomal doxorubicin via the folate receptor in vitro, J. Control. Release 92 (2003) 49–67.
[5] E. Ruoslahti, Drug targeting to specific vascular sites, Drug Discov. Today 7 (2002) 1138–1143.
[6] T.M. Fahmy, P.M. Fong, A. Goyal, W.M. Saltzman, Targeted for drug delivery, Nanotoday 1369 (7021) (2005) 18–26.
[7] A. Kikuchi, S. Sugaya, H. Ueda, K. Tanaka, Y. Aramaki, T. Hara, H. Aramaki, S. Tsuchiya, T. Fuwa, Efficient gene transfer to EGF receptor overexpressing cancer cells by means of EGF-labeled cationic liposomes, Biochem. Biophys. Res. Commun. 227 (1996) 666–671.
[8] C.T.D. Ilarduya, N. Duzgunes, Efficient gene transfer by transferring lipoplexes in the presence of serum, Biochim. Biophys. Acta 1463 (2000) 333–342.
[9] T. Kakudo, S. Chaki, S. Futaki, I. Nakase, K. Akaji, T. Kawakami, K. Maruyama, H. Kamiya, H. Harashima, Transferrin-modified liposomes equipped with a pH-sensitive fusogenic peptide: an artificial viral-like delivery system, Biochemistry 43 (2004) 5618–5628.
[10] A. Gabizon, A.T. Horowitz, D. Goren, D. Tzemach, H. Shmeeda, S. Zalipsky, In vivo fate of folate-targeted polyethylene–glycol liposomes in tumor bearing mice, Clin. Cancer Res. 9 (2003) 6551–6559.
[11] S.H. Kim, J.K. Kim, S.J. Lim, J.S. Park, M.K. Lee, C.K. Kim, Folate-tethered emulsion for the target delivery of retinoids to cancer cells, Eur. J. Pharm. Biopharm. 68 (2008) 618–625.
[12] J.E. Schroeder, I. Shweky, H. Shmeeda, U. Banin, A. Gabizon, Folate-mediated tumor cell uptake of quantum dots entrapped in lipid nanoparticles, J. Control. Release 124 (2007) 28–34.
[13] S.B.A. Jennifer, J.L. Robert, Targeted drug delivery via the folate receptor, Adv. Drug Delivery Rev. 41 (2000) 147–162.
[14] Z.P. Zhang, S.H. Lee, S.S. Feng, Folate-decorated poly(lactide-co-glycolide)-vitamin E TPGS nanoparticles for targeted drug delivery, Biomaterials 28 (2007) 1889–1899.
[15] C.P. Leamon, J.A. Reddy, Folate-targeted chemotherapy, Adv. Drug Delivery Rev. 56 (2004) 1127–1141.
[16] J. Pan, S.S. Feng, Targeting and imaging cancer cells by folate-decorated, quantum dots(QDs)-loaded nanoparticles of biodegradable polymers, Biomaterials 30 (2009) 1176–1183.
[17] J. Pan, S.S. Feng, Targeted delivery of paclitaxel using folate-decorated poly(lactide)-vitamin E TPGS nanoparticles, Biomaterials 29 (2008) 2663–2672.
[18] T. Yoshizawa, Y. Hattori, M. Hakoshima, K. Koga, Y. Maitani, Folate-linked lipid-based nanoparticles for synthetic siRNA delivery in KB tumor xenografts, Eur. J. Pharm. Biopharm. 70 (2008) 718–725.
[19] Y.K. Lee, Preparation and characterization of folic acid linked poly(L-glutamate) nanoparticles for cancer targeting, Macromol. Res. 14 (2006) 387–393.
[20] E.K. Park, S.Y. Kim, S.B. Lee, Y.M. Lee, Folate-conjugated methoxy poly(ethylene glycol)/poly(epsilon-caprolactone) amphiphilic block copolymeric micelles for tumor-targeted drug delivery, J. Control. Release 109 (2005) 158–168.
[21] R. Gref, A. Domb, P. Quellec, T. Blunk, R.H. Muller, J.M. Verbavatz, R. Langer, The controlled intravenous delivery of drugs using PEG-coated sterically stabilized nanospheres, Adv. Drug Delivery Rev. 16 (2–3) (1995) 215–233.
[22] H.S. Yoo, T.G. Park, Folate receptor targeted biodegradable polymeric doxorubicin micelles, J. Control. Release 96 (2) (2004) 273–283.
[23] H. Shmeeda, L. Mak, D. Tzemach, P. Astrahan, M. Tarshish, A. Gabizon, Intracellular uptake and intracavitary targeting of folate-conjugated liposomes in a mouse lymphoma model with up-regulated folate receptors, Mol. Cancer Ther. 5 (4) (2006) 818–824.
[24] H.Y. Li, J. Chang, In vitro degradation of porous degradable and bioactive PHBV/wollastonite composite scaffolds, Polym. Degrad. Stab. 87 (2005) 301–307.
[25] H.Y. Li, J. Chang, Preparation, characterization and in vitro release of gentamicin from PHBV/wollastonite composite microspheres, J. Control. Release 10 (2005) 463–473.
[26] L.Q. Zhao, J.F. Xiao, T. Feng, H.B. Wang, Synthesis of poly (3-hydroxybutyrate-co-3-hydroxyoctanoate) by a *Sinorhizobium fredii* strain, Lett. Appl. Microbiol. 42 (4) (2006) 344–349.
[27] Y.F. Dong, H. Xie, Y. Guo, C. Zhang, S.Y. Ma, Y.P. Zhao, L.Q. Zhao, Biocompatibility of poly(3-hydroxybutyrate-co-hydroxyocatanoate), J. Clin. Rehab. Tissue Eng. Res. 12 (10) (2008) 1870–1872.
[28] Y. Guo, Y.F. Dong, Z. Chen, L.Q. Zhao, Study of P(HB-HO) as scaffold for bone tissue engineering, J. Funct. Mater. 3 (40) (2009) 459–466.
[29] X.B. Xiong, Z.S. Ma, R. Lai, A. Lavasanifar, The therapeutic response to multifunctional polymeric nano-conjugates in the targeted cellular and subcellular delivery of doxorubicin, Biomaterials 31 (2010) 757–768.
[30] Y. Tang, A.J. McGoron, Combined effects of laser-ICG photothermotherapy and doxorubicin chemotherapy on ovarian cancer cells, J. Photochem. Photobiol. B: Biol. 97 (2009) 138–144.
[31] F.A. Fornari, J.K. Randolph, J.C. Yalowich, M.K. Ritke, D.A. Gewirtz, Interference by doxorubicin with DNA unwinding in MCF-7 breast tumor cells, Mol. Pharmacol. 45 (1994) 649–656.
[32] R.J. Lee, P.S. Low, Folate-mediated tumor cell targeting of liposome-entrapped doxorubicin in vitro, Biochim. Biophys. Acta 1233 (1995) 134–144.
[33] H.Z. Zhao, L.Y.L. Yung, Selectivity of folate conjugated polymer micelles against different tumor cells, Int. J. Pharm. 349 (2008) 256–268.
[34] Y. Sheng, C.S. Liu, Y. Yuan, X.Y. Tao, F. Yang, X.Q. Shan, H.J. Zhou, F. Xu, Long-circulating polymeric nanoparticles bearing a combinatorial coating of PEG and water-soluble chitosan, Biomaterials 30 (2009) 2340–2348.
[35] A.G. Coombes, M.K. Yeh, E.C. Lavelle, S.S. Davis, The control of protein release from poly(DL-lactide co-glycolide) microparticles by variation of the external aqueous phase surfactant in the water-in oil-in water method, J. Control. Release 52 (1998) 311–320.
[36] Y.T. Liu, K. Li, J. Pan, B. Liu, S.S. Feng, Folic acid conjugated nanoparticles of mixed lipid monolayer shell and biodegradable polymer core for targeted delivery of Docetaxel, Biomaterials 31 (2010) 330–338.
[37] G.Y. Xiang, J. Wu, Y.H. Lu, Z.L. Liu, R.J. Lee, Synthesis and evaluation of a novel ligand for folate-mediated targeting liposomes, Int. J. Pharm. 356 (2008) 29–36.
[38] R.G. Anderson, Potocytosis: sequestration and transport of small molecules by caveolae, Science 255 (5043) (1992) 410–411.
[39] Y.H. Zhang, L.L. Guo, R.W. Roeske, A.C. Antony, H.N. Jayaram, Pteroyl-γ-glutamate-cysteine synthesis and its application in folate receptor-mediated cancer cell targeting using folate-tethered liposomes, Anal. Biochem. 332 (2004) 168–177.
[40] K.A. Janes, M.P. Fresneau, A. Marazuela, A. Fabra, M.J. Alonso, Chitosan nanoparticles as delivery systems for doxorubicin, J. Control. Release 73 (2001) 255–267.